RSC Advances

PAPER

View Article Online
View Journal | View Issue



Cite this: *RSC Adv.*, 2018, **8**, 17073

# A series of water-soluble photosensitizers based on 3-cinnamoylcoumarin for *in vitro* antimicrobial photodynamic inactivation†

Zhiyuan Sun,‡[ac] Shaona Zhou,‡[b] Haixia Qiu,[b] Ying Gu[b] and Yuxia Zhao *[a]

Received 24th March 2018
Accepted 19th April 2018

DOI: 10.1039/c8ra02557f

rsc.li/rsc-advances

A series of novel water-soluble photosensitizers (PSs; **M1**–**M5**) based on 3-cinnamoylcoumarin derivatives, incorporating carboxylic acid salt (**M1**, **M2**), pyridine salt (**M3**, **M4**) and quaternary ammonium salt (**M5**) groups, were designed and synthesized. Their photophysical and photochemical properties and *in vitro* antimicrobial photodynamic inactivation (PDI) were investigated. **M2**, modified with two carboxylic acid salts, was unstable in phosphate-buffered saline (PBS). The four other PSs all showed higher binding/uptake to methicillin-resistant *Staphylococcus aureus* (MRSA), *A. baumannii* and *C. albicans* compared with the clinical drug methylene blue (**MB**), except for **M1** to *A. baumannii*. Furthermore, the three cationic PSs (**M3**–**M5**) exhibited equivalent antibacterial PDI efficacies against MRSA and *A. baumannii* compared with **MB**. The antifungal efficacies of **M4** and **M5** to *C. albicans* were both significantly higher than that of **MB**, especially for **M5**, indicating that the quaternary ammonium-salt-modified coumarin derivative has substantial potential for antifungal PDI.



## Introduction

Since their discovery in the early 20th century, antibiotics have been widely used to treat a variety of infectious diseases in clinical practice all over the world.[1–3] However, with the extensive use of antibiotics, many drug-resistant or multidrug-resistant bacteria, even superbacteria, have emerged.[4,5] Consensus has now been reached on the importance of reducing the abuse of antibiotics and finding new methods of treating infection diseases.[6–9] Antimicrobial photodynamic inactivation (PDI) uses light to excite a disease-localized photosensitizer (PS) to generate reactive oxygen species (ROS), such as singlet oxygen ($^1O_2$), which can inactivate bacteria, viruses and fungi *in situ*.[10–12] Unlike antibiotics, ROS has strong oxidizing properties with respect to all organic substrates, thus avoiding the problem of drug resistance.[13–15]

Because of the wide variety of microorganisms, there is no clear guide for the selection of PSs for antimicrobial PDI at present. Generally, the outer walls of Gram-positive bacteria are relatively porous, so can readily be penetrated by cationic, anionic, neutral or nonionic PSs.[16] Gram-negative bacteria have an additional and more negatively charged outer layer, which serves as a barrier to prevent the entry of outer species,[17] meaning that only cationic PSs can easily be taken up. However, fungi are different from bacteria. Although fungi have an even thicker negatively charged outer wall than Gram-negative bacteria, anionic PSs still can inactivate them effectively.[18] The available evidence shows that antifungal photodynamic therapy (PDT) involves more complex mechanisms, such as the presence of drug efflux pumps, the induction of enzymes and the formation of biofilms.[19,20]

In our previous work, a series of PSs modified by poly(ethylene glycol) (PEG), pyridinium or carboxylic acid salt based on benzylcyclopentanone were synthesized and investigated.[21] The results showed that pyridinium- and carboxylic-acid-salt-modified PSs both had better antimicrobial PDI efficacies.[22] Additionally, quaternary ammonium-salt-modified PSs have been used as antibacterial agents for a long time, and most could effectively inactivate bacteria.[23–25] Coumarin is a natural substance found in many plants.[26] Many clinical drugs contain coumarin or its derivatives.[27,28] In cancer chemotherapy, coumarin and 7-hydroxycoumarin act as cytostatic agents against renal cell carcinoma.[29,30] Furthermore, coumarins exhibit potent antitumor activities at different stages of cancer formation through various mechanisms, such as inducing cell apoptosis or inhibiting DNA-associated enzymes.[31] In antitumor PDT, it was also proved that coumarin derivatives have good curative effects.[32,33]

In this article, we designed and synthesized five PSs based on 3-cinnamoylcoumarin derivatives through introduction of carboxylic acid salt (**M1** and **M2**), cationic pyridinium salt (**M3** and **M4**) and quaternary ammonium salt (**M5**) groups. Their

[a]*Technical Institute of Physics and Chemistry, Chinese Academy of Sciences, Beijing 100190, P. R. China. E-mail: yuxia.zhao@mail.ipc.ac.cn; Tel: +86 10 82543569*

[b]*Department of Laser Medicine, Chinese PLA General Hospital, Beijing, 100853, P. R. China*

[c]*University of Chinese Academy of Sciences, Beijing 100049, P. R. China*

† Electronic supplementary information (ESI) available. See DOI: 10.1039/c8ra02557f

‡ These authors contributed equally to this work.

photophysical and photochemical properties and *in vitro* antimicrobial PDI toward Gram-positive bacteria methicillin-resistant *Staphylococcus aureus* (MRSA), negative bacteria *A. baumannii* and fungus *C. albicans* were investigated.

# Experimental

### Synthesis and characterization

The synthetic routes towards **M1–M5** are shown in Fig. 1. 3-Acetyl-7-(dimethylamino)-2*H*-chromen-2-one (**1**) and 3-(ethyl(4-formylphenyl)amino) propanoic acid (**2**) were synthesized according to our previous work.[33] 4-Aminobenzaldehyde (**3**), 2-(ethyl(-phenyl)amino)ethanol (**6**), 2,2′-(phenylazanediyl) diethanol (**9**) and 4-(dimethylamino)benzaldehyde (**12**) were purchased from Energy Chemical. All targeted compounds were obtained by an initial high-yield aldol reaction between 3-acetyl-7-(dimethylamino)-2*H*-chromen-2-one and the corresponding *p*-aminobenzaldehyde, followed by the modification of different anions or cations. Synthetic details and characterization data are provided in ESI.†

### Instruments

$^1$H nuclear magnetic resonance (NMR) spectra were recorded on a Bruker AV400 (400 MHz) spectrometer with deuterated reagents, $CDCl_3$ or $D_2O$, using tetramethylsilane as an internal standard. Mass spectra were measured using Bruker APEX 7.0E. Ultraviolet-visible (UV-Vis) spectra were measured using a Hitachi U-3900 spectrophotometer. Steady-state fluorescence was carried out on a Hitachi F-4500 spectrometer. Phosphate-buffered saline (PBS) buffer solution (0.01 M sodium phosphate, pH = 7.2–7.4) was purchased from Solarbio. Other chemical reagents were from Energy Chemical or J&K chemical Ltd. MRSA, *A. baumannii* and *C. albicans* were provided by Chinese PLA General Hospital.

### Singlet oxygen quantum yields ($\Phi_\Delta$)

The singlet oxygen quantum yield ($\Phi_\Delta$) was determined using Rose Bengal (**RB**) as the reference with a yield of 0.47 in dimethylformamide (DMF).[34] 1,3-Diphenylisobenzofuran (DPBF) was used as the scavenger.[35] Mixed solutions of PSs (**M1–M5** or **RB**) and DPBF were prepared. The concentrations of all solutions were adjusted to the same absorbance (0.1) at 473 nm, and the initial concentration of DPBF was consistent. To ensure the saturation of air, all solutions were stirred vigorously during the experimental procedure. The bleaching of the absorption band of DPBF in each solution at 415 nm was monitored under the irradiation of a 473 nm diode laser. The DPBF solution alone was also irradiated to diminish the errors origin from the photo-activation. The $\Phi_\Delta$ of each PS was calculated from the slope of the decay curve.

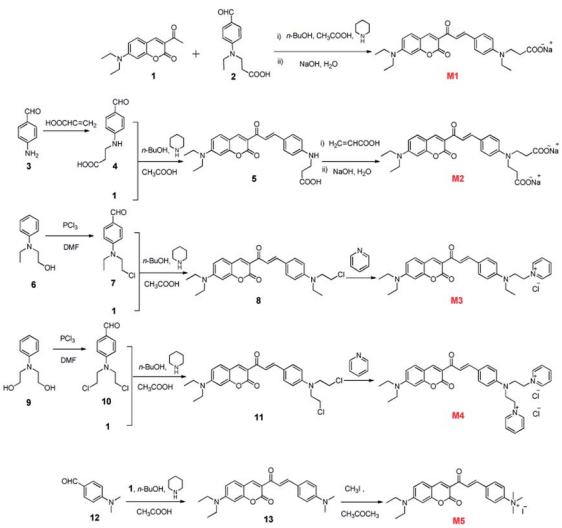


Fig. 1 Synthetic routes to targeted PSs **M1–M5**.

### The uptakes of PSs by microorganism cells

The binding of **M1**, **M3**, **M4** and **M5** to the three strains was measured as previously described.[36,37] Briefly, the concentrations of bacteria or fungus were maintained at McF = 0.5, $10^8$ cells per mL for a bacteria suspension and $10^6$ cells per mL for a fungus suspension with 20 μM PSs. After 1 h of incubation in the dark at room temperature, the suspension was centrifuged at 5000 rpm for 10 min to harvest the bacteria. The obtained bacteria were washed with PBS three times and then lysed with lysozyme (100 μg $mL^{-1}$) for 1 h, followed by sonication for 2 h at 37 °C. The lysed bacterial solution was centrifuged again to obtain the supernatant. The fluorescence intensities of the samples were measured for the different strains. Then the uptakes of various PSs were calculated according to the standard curve.

### *In vitro* antimicrobial PDI

In the PDI group (PS + laser), MRSA and *A. baumannii* ($\sim10^8$ colony-forming unit [CFU] $mL^{-1}$) and *C. albicans* cells ($\sim10^6$ CFU $mL^{-1}$) were incubated with PSs at different concentrations (2.5, 5, 7.5, 10 and 25 μM) for 1 h in the dark and then irradiated under a laser with an exposure dose of 24 J $cm^{-2}$ (irradiated for 10 min by a laser with 40 mW $cm^{-2}$ power density, 457 nm for **M1**, **M3–M5** and 630 nm for methylene blue (**MB**) as the reference). A blank group and a laser group were also included. Incubation and illumination were carried out in 96-well plates (Costar, USA) with 40 μL of mixtures in each well. The viability of the microbial cells was determined by the dilution plating method, as described previously.[38] In brief, 10 μL aliquots of each sample were serially diluted and spread over the surfaces of Sabouraud's dextrose agar plates. All plates were aerobically incubated in an incubator for 24 h. $\log_{10}$ reductions in microbial cells were compared with the untreated control. All experiments were performed three times.

# Results and discussion

### Solubility and octanol–water partition coefficient

The UV-Vis absorption spectra and fluorescence emission spectra of PSs **M1–M5** in PBS are shown in Fig. 2, and their corresponding data are listed in Table 1. All of these PSs have a strong charge transfer (CT) absorption peak at around 470–490 nm. For each PS, both the absorbance maximum $\lambda_{max}^{abs}$ and

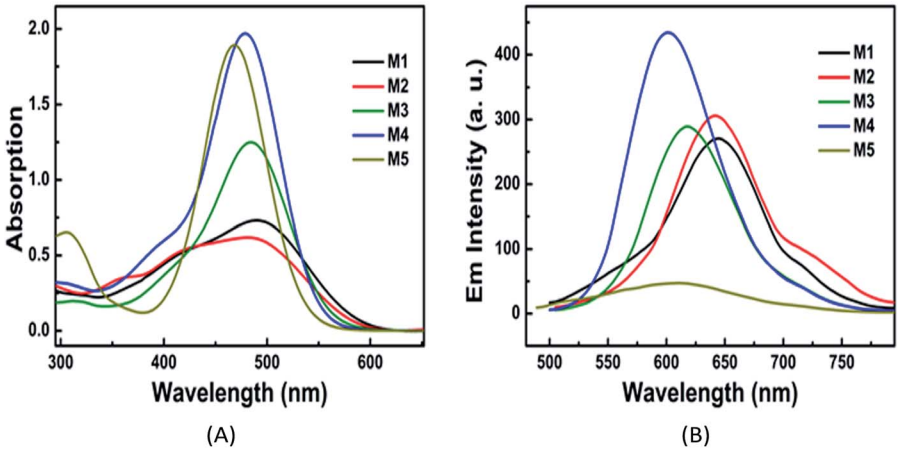


Fig. 2 Absorption (A) and fluorescence (B) spectra of PSs **M1–M5** in PBS ($5.0 \times 10^{-5}$ mol $L^{-1}$).

the fluorescence emission maximum ($\lambda_{max}^{fl}$) in PBS present red-shifts compared with the data in DMF, which can be ascribed to the solvent effects of the reduction of excited state energy in polar proton solvents. The octanol–water partition coefficient (log *P*) are 1.49, −1.20, 0.05, −0.48 and 0.11 for **M1–M5**, respectively. These results indicate that the water solubility of these PSs is enhanced with the increase in the number of pyridinium or carboxylic acid salts. Additionally, the $\Phi_\Delta$ of PSs **M1–M5** were determined as 0.22, 0.10, 0.06, 0.15, and 0.16, respectively, in DMF, which are acceptable for PDT. However, the data in PBS could not be obtained due to the fast decay of singlet oxygen in water or PBS.[35]

## Photostability

The photostability of these PSs was studied under irradiation of a 473 nm laser. As shown in Fig. 3, compared with the four other PSs, **M2** was bleached 15% after 120 s. Additionally, even when kept in the dark, the PBS solution of **M2** was still unstable after 8 h, and was therefore excluded in the follow-up *in vitro* experiments.

## The binding/uptake of PSs by bacteria and fungus cells

The binding/uptake amounts of these PSs by bacteria (MRSA and *A. baumannii*) and fungus (*C. albicans*) were tested. As shown in Fig. 4, **M1** and **M3–M5** can be uptaken more efficiently by the three strains compared with **MB**, which has almost no clear uptake of fluorescence signal. The reason may be ascribed to the good water solubility of **MB** (log $P = -0.96$ (ref. 39 and 40)), which affects its penetration in lipid cell membranes. Moreover, the intakes of **M1**, **M3–M5** by *C. albicans* (665–3320 pmol/$10^6$ cells) are somewhat larger than the corresponding amounts taken by bacteria (2–118 pmol/$10^6$ cells), which is probably because of the larger size of the *Candida* species, about 25–50 times of the bacteria size.[41] For the negatively charged cell walls, the cellular intakes of cationic PSs **M3** and **M5** by both bacteria and fungus are much higher than the corresponding amounts of anionic PS **M1**, such as 118 pmol/$10^6$ cells of **M5** *versus* 38 pmol/$10^6$ cells of **M1** in the MRSA group and 2260 pmol/$10^6$ cells of **M3** *versus* 665 pmol/$10^6$ cells of **M1** in the *C. albicans* group. The cellular uptake of **M1** and **M4** by MRSA and *C. albicans* are similar, while the cellular uptake of **M1** by *A. baumannii* is obviously lower than that of **M4**. These results all

Table 1 Photophysical and photochemical parameters of PSs **M1–M5** in different solvents[a]

| Com | Solvent | log *P* | $\lambda_{max}^{abs}$ (nm) | $\varepsilon_{max}$ ($10^4$ $M^{-1}$ $cm^{-1}$) | $\lambda_{max}^{fl}$ (nm) | $\Delta\nu_{ss}$ ($10^{-4}$ $nm^{-1}$) | $\Phi_f$ | $\Phi_\Delta$ |
|---|---|---|---|---|---|---|---|---|
| **M1** | DMF | 1.49 | 469 | 1.63 | 551 | 3.17 | 0.018 | 0.22 |
| | PBS | | 490 | 1.21 | 641 | 4.81 | 0.0023 | — |
| **M2** | DMF | −1.20 | 437 | 1.98 | 566 | 5.22 | 0.0087 | 0.10 |
| | PBS | | 486 | 1.48 | 643 | 5.02 | 0.0031 | — |
| **M3** | DMF | 0.05 | 473 | 3.46 | 602 | 4.53 | 0.0039 | 0.06 |
| | PBS | | 485 | 2.60 | 618 | 4.44 | 0.0036 | — |
| **M4** | DMF | −0.48 | 470 | 5.15 | 529 | 2.37 | 0.011 | 0.15 |
| | PBS | | 481 | 4.50 | 609 | 4.37 | 0.0039 | — |
| **M5** | DMF | 0.11 | 464 | 3.94 | 559 | 3.66 | 0.0098 | 0.16 |
| | PBS | | 470 | 3.86 | 615 | 5.01 | 0.0022 | — |

[a] log *P* is the octanol–water partition coefficient; $\lambda_{max}^{abs}$ is the absorption band maximum; $\varepsilon_{max}$ is molar absorption coefficient at $\lambda_{max}^{abs}$; $\lambda_{max}^{fl}$ is fluorescence emission maximum; $\Delta\nu_{ss}$ is the Stokes shift; $\Phi_f$ is fluorescence quantum yield; $\Phi_\Delta$ is singlet oxygen quantum yield measured by photochemical trap method.

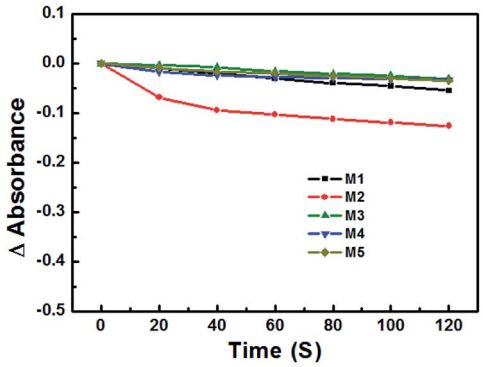


Fig. 3 Photostability of M1–M5 with irradiation time in DMF solution.

indicate that the cationic PSs **M3–M5** have good potential in antimicrobial PDI. Compared with **M3** and **M5**, the binding/uptake of **M4** is lower, which indicates that the charge is not the only determinant. According to our previous report,[22] the cellular uptake also correlated with the log *P* value of PSs. Based on the lower log *P* data of −0.48 for **M4** *versus* 1.49 for **M3** and 0.11 for **M5**, we speculate that the lower binding/uptake of **M4** is due to its enhanced water solubility by introducing two cationic groups.

### *In vitro* antimicrobial PDI

The toxicities of PSs toward the three strains with or without laser irradiation were tested. For the dark toxicity, after incubating the microorganisms with 100 μM PSs **M1**, **M3–M5** or **MB** in the dark for 24 h, the bacteria or the fungus viabilities had no significant decrease in all groups. As shown in Fig. 5, except for the anionic PS **M1**, the cationic PSs **M3–M5** all have equivalent antibacterial PDI efficacies against MRSA and *A. baumannii* compared with the clinical drug **MB**, with an over 3 log CFU $mL^{-1}$ decrease of the bacterial viability when the concentration of **M3–M5** is up to 5 μM. The results correlate well with the cellular uptake and the $\Phi_\Delta$ of the PSs. For *C. albicans*, cationic PSs **M4** and **M5** both exhibited much better antifungal PDI efficacies compared with **MB**, especially for **M5**. There was an over 3 log CFU $mL^{-1}$ decrease of the fungal viability when the concentration of **M5** reached 2.5 μM. However, the antimicrobial PDI efficacy of the anionic PS **M1** was poor, effective only for MRSA, with an over 3 log CFU $mL^{-1}$ decrease of the bacterial viability when its concentration reached 25 μM. For *C. albicans*, the difference may be caused by different mechanisms for various PSs. As mentioned in the introduction, the antifungal PDT process involves more complex mechanisms compared with antibacterial PDT.[42] Unfortunately, until now the specific reasons are still not clear. Additionally, based on the

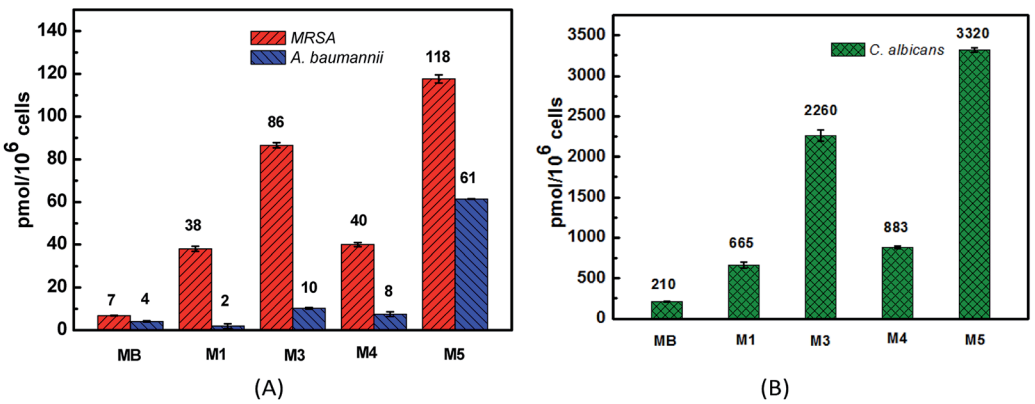


Fig. 4 The cellular uptakes of PSs **M1**, **M3–M5** and reference **MB** by MRSA, *A. baumannii* (A) and *C. albicans* (B).

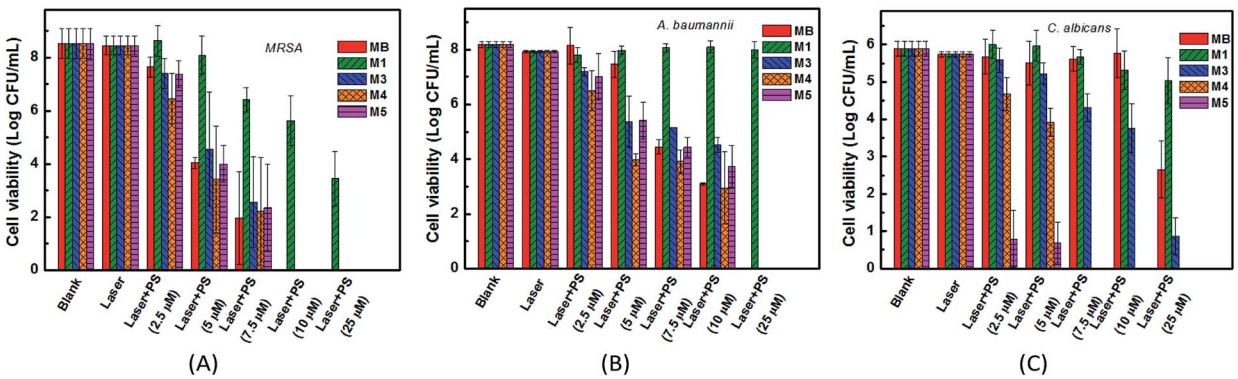


Fig. 5 Relative cell viability of three strains MRSA (A), *A. baumannii* (B) and *C. albicans* (C) after being irradiated with laser (40 mW $cm^{-2}$) for 10 min and then incubated with PSs **M1**, **M3–M5** and **MB** for another 24 h. The error bars denote the standard deviation of three replicates.

 

comparable intake of **M1** and **M4** (Fig. 4), the antimicrobial PDI effect of **M1** is much lower than that of **M4**. Except for the difference between cations and anions, we speculate that the antimicrobial PDI effect of a PS may also correlate with its binding site or subcellular localization, which will be more remarkable when the PS is bound onto an important organelle. Obviously, more studies are required in the future.

## Conclusions

In conclusion, a series of novel water-soluble PSs (**M1–M5**) based on 3-cinnamoylcoumarin derivatives were synthesized, and their properties were investigated. The results show that with the introduction of two carboxylic acid salts, the photostability of the PSs declined. The cationic PSs **M3–M5** exhibited higher binding/uptake to MRSA, *A. baumannii* and *C. albicans* compared with the clinical drug **MB**. Additionally, the *in vitro* experiments showed that three cationic PSs (**M3–M5**) had equivalent antibacterial PDI efficacies against MRSA and *A. baumannii* compared with **MB**. The antifungal PDI efficacies of **M4** and **M5** to *C. albicans* were both much higher than that of **MB**, especially for **M5**. However, anionic PS **M1** was only effective for MRSA. Although the cationic PSs **M4** and **M5** showed an excellent antifungal PDI performance, the specific reasons are still not clear. Further study needs to be carried out to elucidate the mechanism. This work indicates the potential of coumarin derivatives in antimicrobial PDI.

## Conflicts of interest

There are no conflicts of interest to declare.

## Acknowledgements

The work was supported by the National Natural Science Foundation of China (No. 61575208).

## Notes and references

1 A. Rodriguez-Rojas, J. Rodriguez-Beltran, A. Couce and J. Blazquez, *Int. J. Med. Microbiol.*, 2013, **303**, 293–297.
2 A. J. Alanis, *Arch. Med. Res.*, 2005, **36**, 697–705.
3 R. Laxminarayan, A. Duse, C. Wattal, A. K. M. Zaidi, H. F. L. Wertheim, N. Sumpradit, E. Vlieghe, G. L. Hara, I. M. Gould, H. Goossens, C. Greko, A. D. So, M. Bigdeli, G. Tomson, W. Woodhouse, E. Ombaka, A. Q. Peralta, F. N. Qamar, F. Mir, S. Kariuki, Z. A. Bhutta, A. Coates, R. Bergstrom, G. D. Wright, E. D. Brown and O. Cars, *Lancet Infect. Dis.*, 2013, **13**, 1057–1098.
4 R. Ferraz, V. Teixeira, D. Rodrigues, R. Fernandes, C. Prudêncio, J. P. Noronha, Ž. Petrovski and L. C. Branco, *RSC Adv.*, 2014, **4**, 4301–4307.
5 H. Landecker, *Body Soc.*, 2016, **22**, 19–52.
6 X. Ragàs, D. Sánchez-García, R. Ruiz-González, T. Dai, M. Agut, M. R. Hamblin and S. Nonell, *J. Med. Chem.*, 2010, **53**, 7796–7803.
7 T. Dai, Y. Y. Huang and M. R. Hamblin, *Photodiagn. Photodyn. Ther.*, 2009, **6**, 170–188.
8 H. Nikaido, *Science*, 1994, **264**, 382–388.
9 F. S. Felipe, Y. Y. Huang and M. R. Hamblin, *Recent Pat. Anti-Infect. Drug Discovery*, 2013, **8**, 108–120.
10 W. Fan, P. Huang and X. Chen, *Chem. Soc. Rev.*, 2016, **45**, 6488–6519.
11 Y. Shen, A. J. Shuhendler, D. Ye, J. J. Xu and H. Y. Chen, *Chem. Soc. Rev.*, 2016, **45**, 6725–6741.
12 M. R. Hamblin, *Curr. Opin. Microbiol.*, 2016, **33**, 67–73.
13 M. Khurana, H. A. Collins, A. Karotki, H. L. Anderson, D. T. Cramb and B. C. Wilson, *Photochem. Photobiol.*, 2007, **83**, 1441–1448.
14 B. W. Henderson, D. A. Bellnier, W. R. Greco, A. Sharma, R. K. Pandey, L. A. Vaughan and T. J. Dougherty, *Cancer Res. Treat.*, 1997, **57**, 4000–4007.
15 A. V. Kustov, D. V. Belykh, N. L. Smirnova, E. A. Venediktov, T. V. Kudayarova, S. O. Kruchin, I. S. Khudyaeva and D. B. Berezin, *Dyes Pigm.*, 2018, **149**, 553–559.
16 M. A. Pereira, M. A. F. Faustino, J. P. C. Tome, M. G. P. M. S. Neves, A. C. Tome, J. A. S. Cavaleiro, A. Cunha and A. Almeida, *Photochem. Photobiol. Sci.*, 2014, **13**, 680–690.
17 Q. Chen, J. Li, Y. Wu, F. Shen and M. Yao, *RSC Adv.*, 2013, **3**, 13835–13842.
18 G. Jori, C. Fabris, M. Soncin, S. Ferro, O. Coppellotti, D. Dei, L. Fantetti, G. Chiti and G. Roncucci, *Lasers Surg. Med.*, 2006, **38**, 468–481.
19 D. Sanglard, *Curr. Opin. Microbiol.*, 2002, **5**, 379–385.
20 P. Gonzalez-Parraga, J. A. Hernandez and J. C. Arguelles, *Yeast*, 2003, **20**, 1161–1169.
21 Y. Fang, T. Liu, Q. Zou, Y. Zhao and F. Wu, *Sci. Rep.*, 2016, **6**, 28357.
22 Y. Fang, T. Liu, Q. Zou, Y. Zhao and F. Wu, *RSC Adv.*, 2015, **5**, 56067–56074.
23 A. C. Engler, N. Wiradharma, Z. Y. Ong, D. J. Coady, J. L. Hedrick and Y.-Y. Yang, *Nano Today*, 2012, **7**, 201–222.
24 L. Huang, Y. Y. Huang, P. Mroz, G. P. Tegos, T. Zhiyentayev, S. K. Sharma, Z. Lu, T. Balasubramanian, M. Krayer, C. Ruzie, E. Yang, H. L. Kee, C. Kirmaier, J. R. Diers, D. F. Bocian, D. Holten, J. S. Lindsey and M. R. Hamblin, *Antimicrob. Agents Chemother.*, 2010, **54**, 3834–3841.
25 E. R. Kenawy, S. D. Worley and R. Broughton, *Biomacromolecules*, 2007, **8**, 1359–1384.
26 E. Jameel, T. Umar, J. Kumar and N. Hoda, *Chem. Biol. Drug Des.*, 2016, **87**, 21–38.
27 S. Emami and S. Dadashpour, *Eur. J. Med. Chem.*, 2015, **102**, 611–630.
28 F. G. Medina, J. G. Marrero, M. Macias-Alonso, M. C. Gonzalez, I. Cordova-Guerrero, A. G. Teissier Garcia and S. Osegueda-Robles, *Nat. Prod. Rep.*, 2015, **32**, 1472–1507.
29 T. Nasr, S. Bondock and M. Youns, *Eur. J. Med. Chem.*, 2014, **76**, 539–548.
30 G. J. Finn, B. S. Creaven and D. A. Egan, *Eur. J. Pharm. Sci.*, 2005, **26**, 16–25.

31 T. Zhu, Y. Wang, W. Ding, J. Xu, R. Chen, J. Xie, W. Zhu, L. Jia and T. Ma, *Chem. Biol. Drug Des.*, 2015, **85**, 385–393.
32 M. Gangopadhyay, T. Singh, K. K. Behara, S. Karwa, S. K. Ghosh and N. P. Singh, *Photochem. Photobiol. Sci.*, 2015, **14**, 1329–1336.
33 Q. Zou, Y. Fang, Y. Zhao, H. Zhao, Y. Wang, Y. Gu and F. Wu, *J. Med. Chem.*, 2013, **56**, 5288–5294.
34 X.-L. Wang, Y. Zeng, Y.-Z. Zheng, J.-F. Chen, X. Tao, L.-X. Wang and Y. Teng, *Chem.–Eur. J.*, 2011, **17**, 11223–11229.
35 I. E. Kochevar and R. W. Redmond, *Methods Enzymol.*, 2000, **319**, 20–28.
36 K. Mizuno, T. Zhiyentayev, L. Huang, S. Khalil, F. Nasim, G. P. Tegos, H. Gali, A. Jahnke, T. Wharton and M. R. Hamblin, *J. Nanomed. Nanotechnol.*, 2011, **2**, 1–9.
37 A. Rezusta, P. Lopez-Chicon, M. P. Paz-Cristobal, M. Alemany-Ribes, D. Royo-Diez, M. Agut, C. Semino, S. Nonell, M. J. Revillo, C. Aspiroz and Y. Gilaberte, *Photochem. Photobiol.*, 2012, **88**, 613–619.
38 B. D. Jett, K. L. Hatter, M. M. Huycke and M. S. Gilmore, *BioTechniques*, 1997, **23**, 648–650.
39 M. Oz, D. E. Lorke and G. A. Petroianu, *Biochem. Pharmacol.*, 2009, **78**, 927–932.
40 S. J. Wagner, A. Skripchenko, D. Robinette, J. W. Foley and L. Cincotta, *Photochem. Photobiol.*, 1998, **67**, 343–349.
41 P. Calzavara-Pinton, M. T. Rossi, R. Sala and M. Venturini, *Photochem. Photobiol.*, 2012, **88**, 512–522.
42 M. Paardekopper, A. E. V. Gompel, V. J. Steveninck and P. J. Van den Broek, *J. Photochem. Photobiol. B*, 1995, **62**, 561–567.